

Learning to Accelerate Decomposition for Multi-Directional 3D Printing

Chenming Wu¹, Yong-Jin Liu^{1*} and Charlie C.L. Wang^{2*}

Abstract—As a strong complementary of additive manufacturing, multi-directional 3D printing has the capability of decreasing or eliminating the need for support structures. Recent work proposed a beam-guided search algorithm to find an optimized sequence of plane-clipping, which gives volume decomposition of a given 3D model. Different printing directions are employed in different regions so that a model can be fabricated with tremendously less supports (or even no support in many cases). To obtain optimized decomposition, a large beam width needs to be used in the search algorithm, which therefore leads to a very time-consuming computation. In this paper, we propose a learning framework that can accelerate the beam-guided search by using only 1/2 of the original beam width to obtain results with similar quality. Specifically, we train a classifier for each pair of candidate clipping planes based on six newly proposed feature metrics from the results of beam-guided search with large beam width. With the help of these feature metrics, both the current and the sequence-dependent information are captured by the classifier to score candidates of clipping. As a result, we can achieve around 2 times acceleration. We test and demonstrate the performance of our accelerated decomposition on a large dataset of models for 3D printing.

I. INTRODUCTION

Additive manufacturing (AM, also called 3D printing) is a useful technique that can fabricate digital models in an additive manner. Due to its capability of building complex objects rapidly, it has been widely used in many scenarios – from the micro-scale fabrication of bio-structures to on-situ construction of architecture. However, traditional methods using planar layers with fixed 3D printing direction suffer from the need of support structures (shortly called *support* in the following context), which are used to prevent the collapse of material in overhang regions due to gravity. Supports bring in many problems, including hard-to-remove, surface damage and material waste as summarized in [1].

To avoid using large amount of supports, our previous work [2] proposes an algorithm to decompose 3D models into a sequence of sub-components the volume of which can be printed one by one along different directions for different components. Candidates clipping planes are used as a set of samples to define the search space for determining an optimized sequence of decomposition. Different criteria are defined to ensure the feasibility and the manufacturability (e.g., collision-free and no floating region etc.). The most

¹C. Wu and Y.-J. Liu are with the Department of Computer Science and Technology, Tsinghua University, Beijing, China. {wcm15@mails, liuyongjin@mail}.tsinghua.edu.cn

²C.C.L. Wang is with the Department of Mechanical and Automation Engineering The Chinese University of Hong Kong, Hong Kong. cwang@mae.cuhk.edu.hk

* denotes corresponding authors



Fig. 1. A 5-DOF multi-directional 3D printing system that can deposit material along different directions: (left) the printer head can move along x -, y - and z -axes and (right) the working table can rotate around two axes (see the arrows for the illustration of A-axis and C-axis).

important part of this work [2] is a beam-guided search algorithm with progressive relaxation. The benefit of the proposed search algorithm is that it can avoid being stuck in local minimum compared to greedily searching the best result. Beam width $b = 10$ is empirically used to balance the trade-off between computational efficiency and searching effectiveness. Though conducting a parallel implementation running on a computer with Intel(R) Core(TM) i7 CPU (4 cores), the method still results in an average computing time of 6 minutes.

On the other hand, using $b = 10$ is only for the sack of the trading-off. Obviously, a larger b would give us better results since the search space is expanded linearly when b increases – see Fig.2 for an example.

Question: *Can we learn from the results generated by a large beam width so that even a search using a small beam width can produce comparable results?*

Our answer is *yes*. To achieve this goal, we propose to learn a classifier for a pair of candidate clipping planes by using five newly proposed feature metrics. With the help of these feature metrics, both the current and the sequence-dependent information are captured by the classifier to score candidates of clipping. The learning is conducted on the results of beam-guided search with large beam width (i.e., $b = 50$) running on a large dataset of models for 3D printing, *Thingi10k*, recently published by [3]. As a result, we can achieve 2 times acceleration while still keeping the similar quality on the results of volume decomposition.

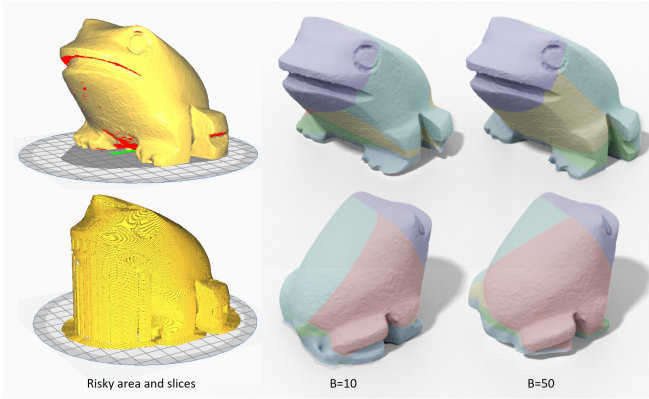


Fig. 2. For a given model (*ID*: 81368 from the *Thing10k* dataset [3]) need large amount of support structures by conventional 3D printing (left), multi-directional 3D printing can significantly reduced the need of support. While increasing the beam width from $B = 10$ (middle) to $B = 50$ (right), the area of region needs to add support can be reduced from 17.34% to 2.64%.

In summary, we make the following contributions:

- A learning-to-accelerate framework that can rank a set of candidate planes that best-fit the optimal results sampled on the large dataset.
- A method to convert the trajectories generated during beam-guided search to pairwise comparisons for training.

The computational efficiency of the proposed work is much better than our previous work [2] while keeping the quality of searching result at the similar level. The implementation of learning-based acceleration presented in this paper together with the solid decomposition approach presented in [2] is available at GitHub¹.

II. RELATED WORK

The problems caused by support have motivated a lot of research effort to reduce the need for supports. There are three significant threads of research towards this goal: 1) proposing better patterns of supports so that the number of supports is smaller than the one generated by vanilla support generator (ref. [4], [5]); 2) segmenting digital models into several pieces, each of which can be built in a support-free or support-effective manner; 3) using high degree-of-freedom (DOFs) robotic systems to automatically change the build direction so that the overhanging regions become safe regions that can be safely fabricated without the need of supports. Here we mainly review the prior work in the last two threads that are most relevant.

A. Segmentation-based Methods

A digital model can be first segmented into different components for fabrication and then assembled back to form the original model. There are a number of methods that have explored to use segmentation to reduce the need of

supports. Hu et al. [6] invented an algorithm to automatically decompose a 3D model into parts in approximately pyramidal shapes to be printed without support. Herholz et al. [7] proposed another algorithm to solve a similar problem by enabling slight deformation during decomposition where each components is in the shape of height-fields. RevoMaker [8] fabricated digital models by 3D printing on top of an existing cubic component, which can rotate itself to fabricate the shape of height-fields. Wei et al. [9] partitioned a shell model into a small number of support-free parts using a skeleton-based algorithm. Muntoni et al. [10] also tackled the problem of decomposing a 3D model into a small set of non-overlapped height field blocks, which can be fabricated by either molding or AM. These methods are mostly algorithmic systems that can be easily incorporated into off-the-shelf manufacturing devices. However, the capability of manufacturing hardware has not been considered in the design of algorithms.

B. Multi-directional and Multi-axis Fabrication

Recent development in robotic systems enable researchers to think about a more flexible AM routine [11]. Adding more DOFs into the process of 3D printing seems promising and has gained a lot of attention. Keating and Oxman [12] proposed to use a 6-DOF manufacturing platform driven by a robotic arm to fabricate the model either in an additive or subtractive manner. Pan et al. [13] rethink the process of CNC machining and proposed a 5-axis motion system to accumulate materials. *On-the-Fly Print* system proposed by Peng et al. [14] is a fast, interactive printing system modified from an off-the-shelf Delta printing device but with two additional DOFs. Based on the same system, Wu et al. [15] proposed an algorithm that can plan the collision-free printing orders of edges for wireframe models.

Industrial robotic arms have been widely used in AM. For example, Huang et al. [16] built up a robotic system for 3D printing wireframe models on a 6-DOF KUKA robotic arm. Dai et al. [17] developed a voxel-growing algorithm for support-free printing digital models using a 6-DOF UR robotic arm. Shembekar et al. [18] proposed a method to fabricate conformal surfaces by collision-free 3D printing trajectories on a 6-DOF robotic arm. To reduce the expense of hardware, a 3 + 2-axis additive manufacturing is also proposed recently [19]. They adopted a flooding algorithm to plan a collision-free and support-free paths. However, this approach can only be applied to tree-like 3D models with simple topology. Volume decomposition based algorithms have been proposed in our prior work (ref. [2], [20]).

C. Learning to Accelerate Search

Searching feasible solution is a common problem in computer science, where most problems with huge search space are difficult to tackle. It is crucial to develop an efficient algorithm to solve search problems. The methodology of incorporating machine learning to accelerate search has been proved to be useful. For example, optimizing a program using different predefined operators is a combinatorial problem,

¹<https://github.com/chenming-wu/pymdp/>

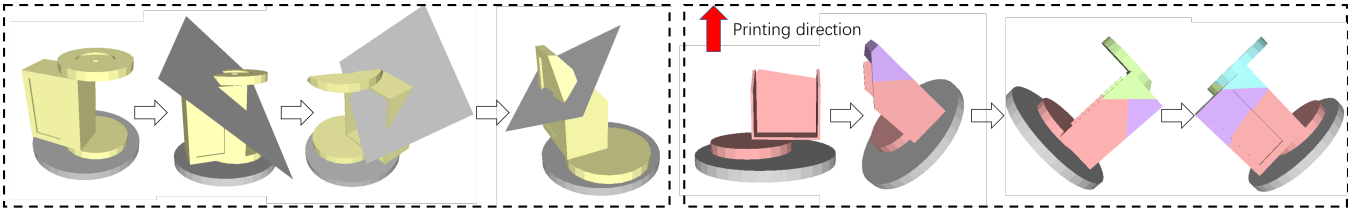


Fig. 3. A sequence of multi-directional 3D printing can be determined by computing a sequence of planar clipping (left), where the inverse order of clipping gives the sequence of multi-directional 3D printing (right). Details can be found in [2].

and it is difficult to search for an optimal solution. The work of Chen et al. [21] learned domain-specific statistical cost models to guide the search of tensor implementations over many possible choices for efficient deep-learning deployments. Recently, Adams et al. [22] improved a beam search algorithm for Halide program optimization. They proposed to learn a cost model to predict runtime that takes the input of the derived features. Similarly, our work also aims at optimizing sequences of operations because applying different cuts in different stages also formulates an ample search space, and different orders matter. A simple but effective method is proposed in this paper.

III. PRELIMINARIES AND DENOTATIONS

This section briefly introduces the idea of the beam-guided algorithm previously proposed in [2].

A. Problem Formulation

Whether fabricating a model \mathcal{M} layer-by-layer needs additional supports can be determined by if *risky faces* exist on the surface of \mathcal{M} . A commonly used definition of identifying a risky face f is

$$e(f, \pi) = \begin{cases} 1 & \mathbf{n}_f \cdot \mathbf{d}_\pi + \sin(\alpha_{max}) > 0, \\ 0 & \text{otherwise.} \end{cases} \quad (1)$$

where \mathbf{d}_π (as the normal of π) gives the printing direction defined by a base plane π , \mathbf{n}_f is the normal of f and α_{max} is the maximal self-supporting angle (ref. [1]). Face f is risky if $e(f, \pi) = 1$ and otherwise it is called *safe*.

In [2], a multi-directional 3D printer is supervised by fabricating a sequence of parts decomposed from \mathcal{M} where:

- N components decomposed from \mathcal{M} satisfies

$$\mathcal{M} = \mathcal{M}_1 \cup \mathcal{M}_2 \cup \dots \cup \mathcal{M}_N = \bigcup_{i=1}^N \mathcal{M}_i \quad (2)$$

with \cup denoting the *union* operator;

- $\{\mathcal{M}_{i=1, \dots, N}\}$ is an ordered sequence that can be collision-freely fabricated with

$$\pi_{i+1} = \mathcal{M}_{i+1} \cap \left(\bigcup_{j=1}^i \mathcal{M}_j \right) \quad (3)$$

being the base plane of \mathcal{M}_{i+1} , where \cap denotes the *intersection* operator;

- π_1 is the working platform of a 3D printer;
- All faces on a sub-region \mathcal{M}_i are *safe* according to \mathbf{d}_{π_i} determined by π_i .

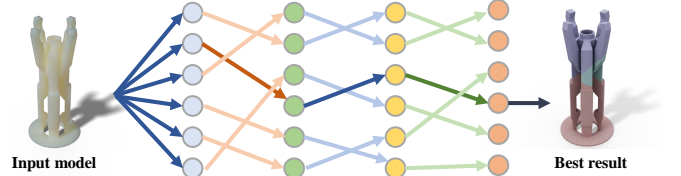


Fig. 4. An example of beam-guided searching trajectories generated in a case with $b = 6$. The trajectory in dark color is the best trajectory τ^* giving the lowest value of J_G . The trajectories shown in light colors are the other trajectories having smaller values of J_G than the one of τ^* .

To tackle this problem, we use half-space plane γ_k to cut 3D models. If every clipped sub-region satisfies the manufacturability criteria, we could use the inverse order of clipping as the sequence of printing for the multi-directional 3D printers (see Fig.3 for an illustration). The printing direction of a sub-part \mathcal{M}_i is determined by the normal of the clipping plane.

We formulate the problem of reducing the area of risky faces on \mathcal{M}_i as a problem that minimizes

$$J_G = \sum_i \sum_{f \in \mathcal{M}_i} e(f, \pi_i) A(f) \quad (4)$$

where $A(f)$ is the area of face f . While minimizing the objective function defined in Eq.(4), we need to ensure the manufacturability of each component.

B. Beam-guided Search

The beam-guided search is to optimize Eq.(4). Considering the manufacturing constraints as well as search efficiency, we define four constraints in beam-guided search.

Criterion I: All faces on \mathcal{M}_i should be self-supported.

Criterion II: The remained model obtained by every clipping should be connected to the printing platform \mathcal{P} .

Criterion III: The physical platform of the printer \mathcal{P} is always below the clipping plane.

Criterion IV: It is always preferred to have a large solid obtained above a clipping plane so that a large volume of solid can be fabricated along one fixed direction.

A beam-guided search algorithm is proposed to guide the search. Beam search [23] is an efficient search technique that has been widely used to improve the results of the best-first greedy search. It builds a search tree that explores the search space by expanding a number of promising nodes (b nodes as *beam width*) instead of the best one greedily (see Fig.4). It integrates the restrictive Criterion I (and its weak form) as

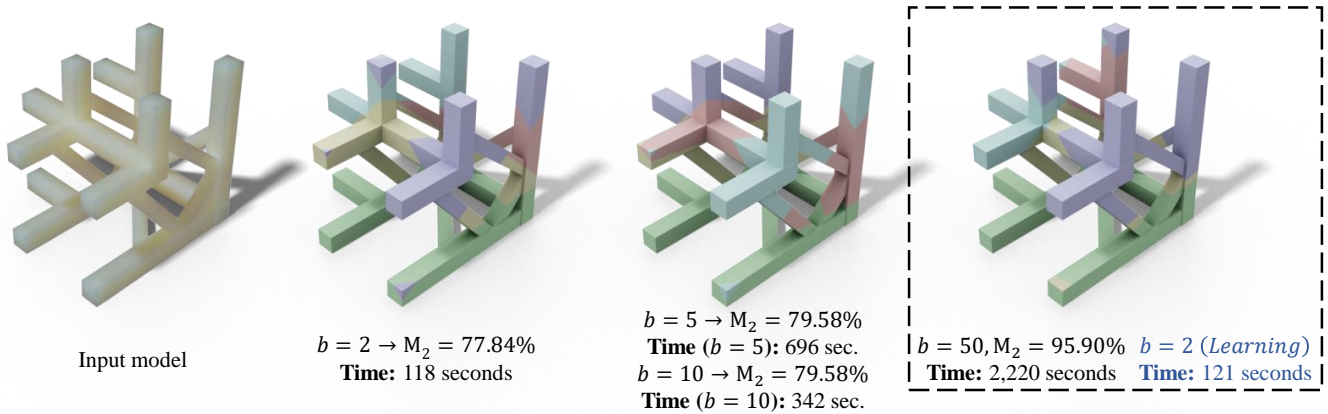


Fig. 5. An example in the *Thingi10k* dataset (ID: 109926). Our learning-based method outperforms the beam-guided search algorithms with a small beam width b . Here, M_2 indicates the percentage of reduced risky area when using multi-directional 3D printing – the higher the better.

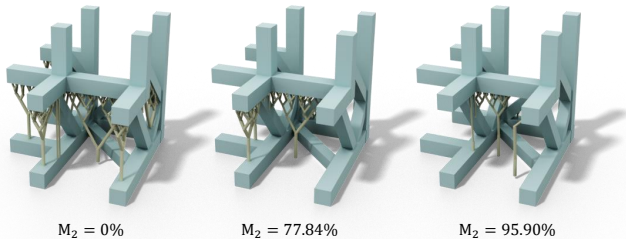


Fig. 6. A visualization on different amounts of support generated using the projected support algorithm in [2]. The decomposition results are from Fig.5.

an objective function to ensure that the beam search is broad enough to include both the local optimum and configurations that may lead to a global optimum. Defining the residual risky area of a model \mathcal{M}_k according to a clipping plane γ as

$$R(\mathcal{M}_k, \gamma) = \sum_{f \in \mathcal{M}_k^+} e(f, \pi(\gamma))A(f), \quad (5)$$

where γ separates \mathcal{M}_k into the part \mathcal{M}_k^+ above γ and the part \mathcal{M}_k^- below γ . The proposed beam-guided search algorithm starts from an empty beam with the most restrictive requirement of $R(\mathcal{M}_k, \gamma) < \delta$, where δ is a threshold progressively increasing from a tiny number (e.g., 0.0001). Candidate clipping planes that satisfy this requirement and remove larger areas of risky faces have higher priority to fill the b beams. If there are still empty beams after the first ‘round’ of filling, we relax δ by letting $\delta = 5\delta$ until all b beams are filled. Detail algorithm can be found in [2].

IV. LEARNING TO ACCELERATE DECOMPOSITION

A. Methodology

The beam-guided algorithm [2] constrains the search space by imposing the manufacturing constraints (Criteria II & III) and the volume heuristic (Criterion IV) while progressively relaxing the selection of ‘best’ candidates (Criterion I). A larger beam width b keeps more less optimal

candidates, which will then have better chance to obtain a globally optimal solution. We conduct an experiment on the Thingi10k dataset to compare different choices of b , and it turns out that the average performance by $b = 50$ is around 17.42% better than the average performance generated by $b = 1$ while it takes more than $36\times$ computing time to obtain those results. One example is given in the right of Fig.5. The experimental results encourage us to explore the feasibility of learning from the underlying experience produced by a large beam width of B , and utilizing the learned policy to guide a more effective search which only keeps a much smaller beam-width b ($b < B$) during the search procedure.

Specifically, given b nodes for configurations kept in the beam, we will be able to obtain thousands of candidates of the next cut. The original method presented in [2] is employed to select the ‘best’ and the relaxed ‘best’ B candidates ($B > b$). Here we will not keep all these B candidates in the beam. Instead, only b candidates are selected from these B candidates, where the selection is conducted with the help of a pair-comparison based classifier $G(\cdot)$ using six enriched feature metrics as input for each candidate clipping. An illustration for this selection procedure can be found in Fig.7. The classifier is constructed by decision-tree based ensemble, which is trained by using the samples learned from conducting beam-guided searches [2] on *Thingi10k* – a large dataset of 3D printing models with a large beam-width $B = 50$.

In the rest of this section, we will first provide the enriched feature metrics. Then, we present the details of the accelerated search algorithm and the method to generate training samples. Lastly, the learning model of classifier is introduced.

B. Featurization of Candidate Clipping

We featurize each candidate cut to a vector consisting of six metrics. The metrics are carefully designed according to the criteria given in Sec. III, which consider both the current and the sequence-dependent information for the configuration of a planar clipping. Note that, it is very important to

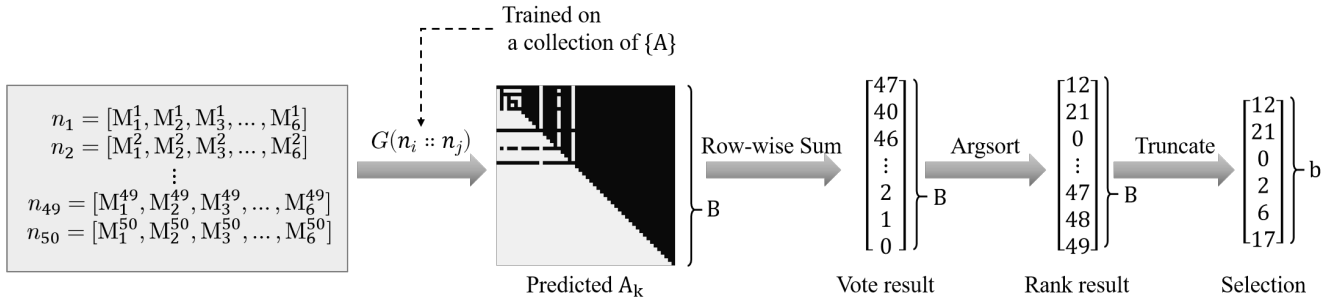


Fig. 7. An example that shows the pipeline of our learning to accelerate decomposition. At each stage, we use a relatively vast $B = 50$ to generate candidate cuts and their metrics. Then we use the trained score function $G(n_i :: n_j)$ to predicate a preference matrix A_k to depict relative priority between pairs of cuts. After that, we convert the predicated A_k to a voting result by row-wise summing and rank the result by arg-sorting. Lastly, we can select the first b cuts (with $b < B$ - e.g., $b = 6$ in this example) from the selection vector for the next-round searching of decomposition.

have metrics to cover the sequence-dependent information (i.e., M_2 and M_6 below). Otherwise, it has trivial chance to learn the strategy of beam-guided search that will not be stuck at local optimum when using large beam width.

Ratio of reduced risky area M_1 : The reduced risky area is essentially the decreased value of Eq.(4). M_1 is defined as the ratio of decreased risk area caused by a candidate clipping plane (the *candidate*) over the value of J_G .

Accumulated ratio of reduced risky area M_2 : Different stages have different values of M_1 , which only reflect a local configuration. We define the sum of M_1 as the accumulated ratio of reduced risky area to describe the situation of a sequence of planning. In short, $M_2 = \sum M_1$.

Processed volume M_3 : The volume of region removed by a clipping plane γ directly determines the efficiency of a cutting plan - larger volume removed per cut leads to less times of clipping. We normalize it to $[0, 1)$ by using the volume of given model $V(\mathcal{M})$.

Distance to platform M_4 : To reflect the requirement on letting the working platform \mathcal{P} always below a clipping plane γ , we define a metric as the minimal distance between γ and \mathcal{P} . M_4 is normalized by using the radius of \mathcal{M} 's bounding sphere.

Distance to fragile regions M_5 : To prevent the generation of fragile regions during 3D printing, we define the minimal distance between a clipping plane γ and all the fragile regions, which can be detected by the method presented in [24]. Again, this distance is normalized by the radius of \mathcal{M} 's bounding sphere.

Accumulated residual risky area M_6 : None of above metric has considered the area that cannot be fully support-free even after decomposition - i.e., having residual risky areas. Here we add a metric to consider the accumulated residual risky area, which is also normalized by the total risky area as $M_6 = \sum R(\mathcal{M}_k, \pi_k) / J_G$.

Without loss of generality, for a candidate clipping in any stage of the planning process, it can use the vector formed by above six metrics to describe its configuration. As illustrated

in Fig.4, each candidate clipping is represented as a node during the beam-guided search. A node n_i is denoted by $n_i = [M_1^i, M_2^i, M_3^i, \dots, M_6^i]$ associated with the six metrics. In this following sub-section, we will introduce the method to select nodes kept in the beam-guided search by using the values of these metrics.

C. Accelerated Search Algorithm

Using the beam-guided search algorithm we can obtain a list of candidate cuts with feature vectors evaluated by six metrics. The beam-guided search algorithm always keeps up to B promising nodes $\mathcal{N}_k = \{n_1^k, \dots, n_B^k\}$ at stage k . We observe that each node n^k may come from different parent nodes from its last stage $k-1$, and n^k may result in different offspring nodes at the next stage $k+1$. This essentially constructs a set of trajectories starting from the input digital model to the globally optimal solution of decomposition (see Fig.4 for an example).

When working on an input mesh \mathcal{M} , we can search many possible trajectories by running the beam-guided search algorithm. Each trajectory τ has a corresponding cost of $J_G(\tau)$. Comparing a pair of nodes $n_a^k \in \tau_A$ and $n_b^k \in \tau_B$ at the same stage k belong to different trajectories τ_a and τ_b , we would have more preference to keep the node n_a^k in the beam than n_b^k when $J_G(\tau_A) < J_G(\tau_B)$ as the trajectory τ_A is more optimal. This is denoted as $n_a^k \triangleright n_b^k$. Therefore, at any stage k , we can always obtain a preference matrix $\bar{A}_k = [A_{a,b}]_{B \times B}$ by letting

$$A_{a,b} = \begin{cases} \text{True} & (n_a \triangleright n_b) \\ \text{False} & (n_a \triangleleft n_b) \end{cases} \quad (6)$$

When a node belongs different trajectories, we always use the one with smallest J_G to update the preference matrix.

Selecting b nodes from the preference matrix \bar{A}_k by voting can have high chance to keep nodes belong to the trajectories with smaller value of J_G in the result of selection. Here the voting is conducted by row-wise summing and then ranking the result of sum by arg-sorting. In our algorithm, we are trying to learn a classifier $G(\cdot)$ that can generate the preference matrix $A_k = [a_{i,j}]$ by using the feature-metrics such that $A_k \approx \bar{A}_k$. Specifically, $a_{i,j} = G(n_i :: n_j)$ with the

input of 12 metrics from two nodes n_i and n_j . With the help of the classifier $G(\cdot)$ learned from searches with large beam-width. The search with smaller beam-width b is expected to generate results with similar quality. See also the illustration of our classifier-based voting step for selecting b nodes out of B candidates given in Fig.7.

D. Pairwise Learning

For an input mesh \mathcal{M} , we can obtain a collection of resultant trajectories by running the beam-guided search algorithm. Each trajectory has a corresponding cost of $J_G(\tau)$. Here we propose a method to convert the trajectories to pairwise samples to be used for learning the classifier $G(\cdot)$. Specifically, a method is developed to sample trajectories obtained from beam-guided search with a large beam width $B = 50$ on a large dataset of 3D printing models.

Our learning method consists of four major steps.

- First, we need to featurize each candidate of clipping to distinguish the differences among the other candidate. Here the six metrics introduced above in Sec. IV-B (i.e., $M_{1,\dots,6}$) are used here.
- Second, we build a dataset made up of these features by running the beam-guided algorithm with a vast beam width of $B = 50$. This step is very time-consuming because of the large B costs more computational resources.
- Third, we convert the trajectories to pairwise comparison samples at every stage of the beam-guided search which describes the relative relationship between two different candidates of clipping. Specifically, given two sets of trajectories \mathcal{T}_A and \mathcal{T}_B of the trajectories that contains n_a^k and n_b^k respectively, we can determine the best trajectories as $\tau_A = \arg \min_{\tau \in \mathcal{T}_A} J_G(\tau)$ and $\tau_B = \arg \min_{\tau \in \mathcal{T}_B} J_G(\tau)$. Then, we define

$$G(n_a^k :: n_b^k) = \begin{cases} 1 & (J_G(\tau_A) < J_G(\tau_B)) \\ 0 & (J_G(\tau_A) \geq J_G(\tau_B)) \end{cases} \quad (7)$$

If a node is not contained in any trajectory, it is regarded as worse than all other nodes that are contained in any trajectory. The training samples are collected from all stages of beam-guided search.

- Finally, we use the pairwise data to train the classifier $G(\cdot)$ by supervised learning.

The resultant classifier $G(\cdot)$ will be used to evaluate every candidate of clipping in our algorithm.

Now we have the dataset constituting of pairwise comparisons for training. Our goal is to train a scoring system on the pairwise dataset to score and rank candidate cuts at each stage of beam-guided search. Once the scoring system is trained, it can be utilized to replace the original sort-and-rank component in the beam-guided algorithm. Our classifier is a decision-tree-based ensemble that constitutes many weak classifiers (as shown in Fig.8) [25]. Detail parameters are given in the section below.

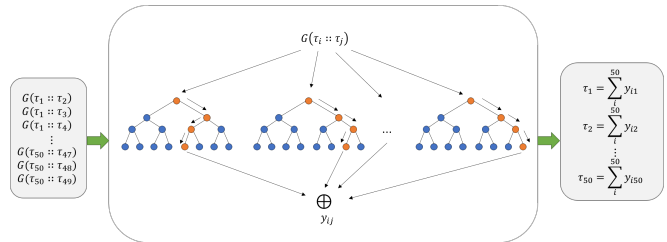


Fig. 8. The boosting-trees-based ensemble is used for learning the classifier in our algorithm.

V. TRAINING AND EVALUATION

A. Dataset Preparation and Training

We implemented the proposed pipeline using C++ and Python, and trained the decision-tree-based ensemble using XGBoost [25]. The trained model and source codes are publicly accessible. The dataset collection phase is conducted on a high-performance server equipped with two Intel E5-2698 v3 CPUs and 128 GB RAM. All other tests are performed on a PC equipped with an Intel Core i7 4790 CPU, NVIDIA Geforce GTX 980 Ti GPU and 24 GB RAM. We use 600 directions sampled on the Gaussian sphere with 1mm intervals to evaluate the metrics. The maximal self-supporting angle is set as $\alpha_{\max} = 45^\circ$.

We trained our model on the *Thing10k* dataset [3] repaired by Hu et al. [26]. Instead of training and evaluating on the whole dataset, we extract a subset of the dataset (2061 models) that satisfies every model in the selected dataset should have a few risky faces that can be processed by our plane-based cutting algorithm. The training dataset for our classifier is built by running the beam-guided search algorithm with $B = 50$. By aforementioned sampling methods, we obtain a dataset with 11.96 million pairs of samples. We split all the dataset to 60% samples for training, 15% samples for validation and 25% data for testing. The decision-tree-based ensemble is trained by using the following parameters.

$$\begin{array}{lll} \text{eta: } 0.1 & \text{gamma: } 0.1 & \text{n. estimator: } 250 \\ \text{max depth: } 10 & \text{reg. alpha: } 1.2 & \text{reg. lambda: } 1.8 \end{array}$$

B. Performance Evaluation on Ranking

In our learning-based acceleration algorithm, we prefer to train a network that shows better precision-at- k (Prec@ k) [27], where k is the beam width we plan to deploy in the accelerated search algorithm. This measure is defined by the fraction of target items out of the first k items. For example, if the actual ranking is $[1, 2, 3, 4, 5]$ and our network gives a ranking as $[1, 3, 2, 5, 4]$, the Prec@ k of $k = 2$ is $\frac{1+0}{2} = 0.5$, but the Prec@ k of $k = 4$ is $\frac{1+1+1+0}{4} = 0.75$.

We use the Prec@ k measure to evaluate the performance of the trained network with different values of k in a range of $[1, 10]$. We also use another widely used statistical measure – mean average precision (MAP) with cut-off [28] to evaluate the performance, which is defined by the averaged Prec@ k score of a ranking over all possible k .

$$MAP(k) = \frac{1}{N} \sum_N \frac{1}{k} \sum_{k'=1}^k Prec@k' \quad (8)$$

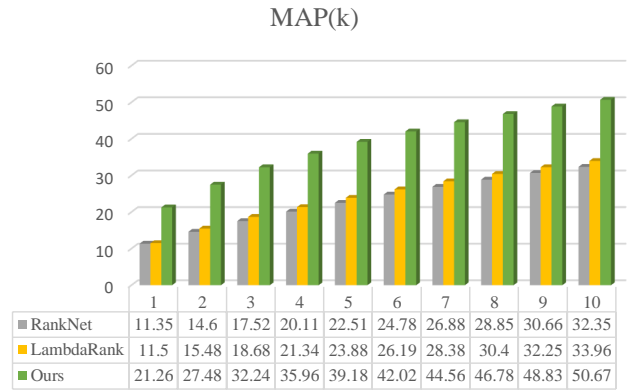
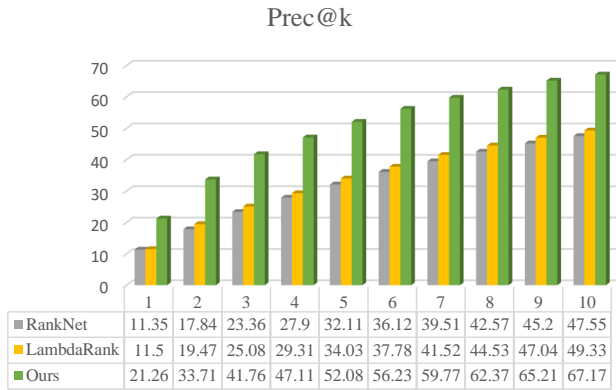


Fig. 9. The comparison of the ranking performance of our method, RankNet and LambdaRank using the same training set and parameters.

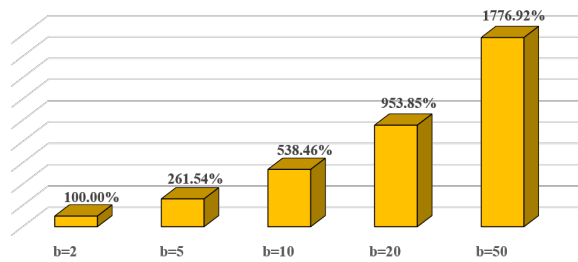


Fig. 10. Computational time when using different beam-width b .

We compare our method with other classic ranking algorithms used in information retrieval, including the listwise approach – LambdaRank [29] and the pairwise approach – RankNet [30]. We use the implementations provided in XGBoost² with the same parameters used for training our scoring system. For training the LambdaRank model, we need to specify the relevance value for each feature, thus we set the relevance values of top 5 features to $[5^2, \dots, 1^2]$ and the ones of the other features to 0. All experimental results are reported in Fig.9. The results show that our method the best performance among all these three approaches.

C. Evaluation on Accelerated Search

The computing time of the beam-guided search algorithm is significantly influenced by the chosen value of beam width b . We first show a comparison of computing times when using different beam widths in Fig.10.

After the training phase is finalized, we now have a scoring systems to rank a set of features evaluated by candidate planes. We replace the simple sort-and-rank module in our beam-guided search algorithm with the classifier and use $b = 2$ and 5 for evaluation. To make the search procedure insensitive to minor overfitting bias, we always check if the best result ranked by the simple sort-and-rank module is in the selected beam. We run both the algorithm with the trained model and the original algorithm by different choices of b

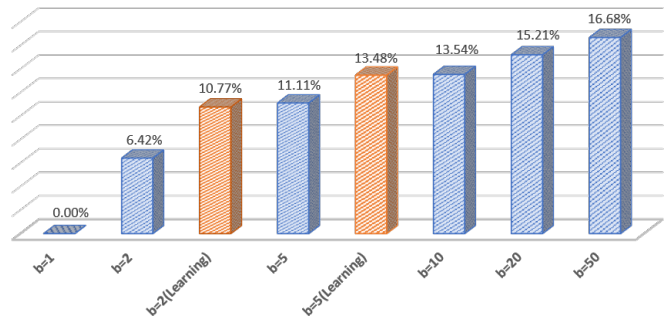


Fig. 11. We use the results generated by the original beam-guided algorithm with $b = 1$ as baseline to compare the performance improvements over different choices of b and our learning-based algorithm.

on the testing dataset (511 models). The statistical result in terms of performance is shown in Fig.11.

The performance comparison (Fig.11) shows that we can use a relatively small b with the trained model to achieve a similar performance generated by a larger b . In other words, the search speed can be accelerated while the searched results are comparative to the ones generated using longer computing time. Meanwhile, we can improve the quality of the results produced by the original algorithm if using the trained model to select cuts. We also observe that there are some cases (e.g., Fig.5) where even a small $b = 2$ with the trained model can produce a high-quality result, which is better than the ones generated by the original beam-guided search algorithm using $b = 2$ and 5 and the same with the ones generated by $b = 20$ and 50.

D. Compare with other classifiers

In our paper, we utilize a boosting-tree-based ensemble for pairwise learning, which is because we find out it provides the best performance. Here we use two neural-network-based classifiers, one is a classic multi-layer perceptron (MLP) consisting of two hidden layers with 24 and 6 hidden units respectively. The other is based on the same architecture but with additional recurrent hidden units to facilitate multi-stage predictions, and we set the dimension of the hidden vector as 3. Note that we train the recurrent neural network using

²<https://github.com/dmlc/xgboost/tree/master/demo/rank>

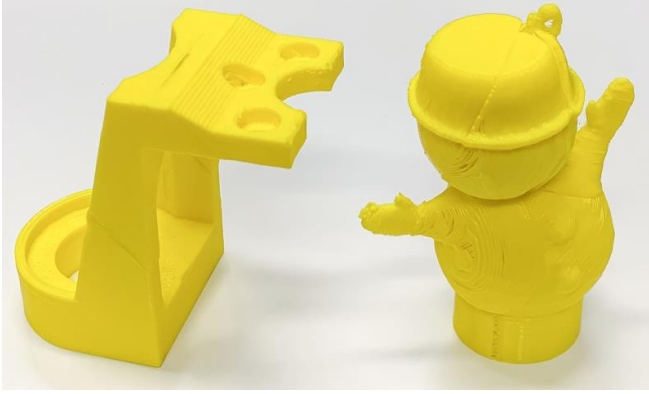


Fig. 12. Two models fabricated by our multi-directional 3D printer – the hardware given in Fig.1.

different data pre-processing as it needs inter-stage information. Our ensemble shows the best performance among the three. As shown in 11, our method gives 10.77% and 13.48% improvements on $b = 2$ and 5, while the MLP method gives 9.21% and 11.87% and the classifier with recurrent hidden units gives 9.34% and 12.02%.

VI. CONCLUSION

This paper presents an accelerated decomposition algorithm for multi-directional printing that can reduce the need of support structures. The proposed method utilizes learning-based method to train a decision-tree-based ensemble that can score the candidates of clipping. We use the trained classifier to guide the search to replace the simple sort-and-rank module in the beam-guided search algorithm. The computing time is reduced to 1/2 while keeping the results with similar quality. The experimental results demonstrate the effectiveness of our proposed method. We provide an easy-to-use python package and make the source code publicly accessible.

REFERENCES

- [1] K. Hu, S. Jin, and C. C. L. Wang, "Support slimming for single material based additive manufacturing," *Computer-Aided Design*, vol. 65, pp. 1–10, 2015.
- [2] C. Wu, C. Dai, G. Fang, Y.-J. Liu, and C. C. Wang, "General support-effective decomposition for multi-directional 3-d printing," *IEEE Transactions on Automation Science and Engineering*, 2019.
- [3] Q. Zhou and A. Jacobson, "Thing10k: A dataset of 10,000 3d-printing models," *arXiv preprint arXiv:1605.04797*, 2016.
- [4] J. Vanek, J. A. Galicia, and B. Benes, "Clever support: Efficient support structure generation for digital fabrication," in *Computer Graphics Forum*, vol. 33, no. 5. Wiley Online Library, 2014, pp. 117–125.
- [5] J. Dumas, J. Hergel, and S. Lefebvre, "Bridging the gap: Automated steady scaffolding for 3d printing," *ACM Trans. Graph.*, vol. 33, no. 4, pp. 98:1–98:10, July 2014.
- [6] R. Hu, H. Li, H. Zhang, and D. Cohen-Or, "Approximate pyramidal shape decomposition," *ACM Trans. Graph.*, vol. 33, no. 6, pp. 213:1–213:12, 2014.
- [7] P. Herholz, W. Matusik, and M. Alexa, "Approximating free-form geometry with height fields for manufacturing," *Computer Graphics Forum*, vol. 34, no. 2, pp. 239–251, 2015.
- [8] W. Gao, Y. Zhang, D. C. Nazzetta, K. Ramani, and R. J. Cipra, "RevoMaker: Enabling multi-directional and functionally-embedded 3D printing using a rotational cuboidal platform," in *Proceedings of the 28th Annual ACM Symposium on User Interface Software and Technology*, 2015, pp. 437–446.
- [9] X. Wei, S. Qiu, L. Zhu, R. Feng, Y. Tian, J. Xi, and Y. Zheng, "Toward support-free 3D printing: A skeletal approach for partitioning models," *IEEE Transactions on Visualization and Computer Graphics*, vol. 24, no. 10, pp. 2799–2812, Oct 2018.
- [10] A. Muntoni, M. Livesu, R. Scateni, A. Sheffer, and D. Panozzo, "Axis-aligned height-field block decomposition of 3D shapes," *ACM Trans. Graph.*, 2018.
- [11] P. Urhal, A. Weightman, C. Diver, and P. Bartolo, "Robot assisted additive manufacturing: A review," *Robotics and Computer-Integrated Manufacturing*, vol. 59, pp. 335–345, 2019.
- [12] S. Keating and N. Oxman, "Compound fabrication: A multi-functional robotic platform for digital design and fabrication," *Robotics and Computer-Integrated Manufacturing*, vol. 29, no. 6, pp. 439–448, 2013.
- [13] Y. Pan, C. Zhou, Y. Chen, and J. Partanen, "Multitool and multi-axis computer numerically controlled accumulation for fabricating conformal features on curved surfaces," *ASME Journal of Manufacturing Science and Engineering*, vol. 136, no. 3, 2014.
- [14] H. Peng, R. Wu, S. Marschner, and F. Guimbretière, "On-the-fly print: Incremental printing while modelling," in *Proceedings of the 2016 CHI Conference on Human Factors in Computing Systems*. ACM, 2016, pp. 887–896.
- [15] R. Wu, H. Peng, F. Guimbretière, and S. Marschner, "Printing arbitrary meshes with a 5dof wireframe printer," *ACM Trans. Graph.*, vol. 35, no. 4, p. 101, 2016.
- [16] Y. Huang, J. Zhang, X. Hu, G. Song, Z. Liu, L. Yu, and L. Liu, "Framefab: robotic fabrication of frame shapes," *ACM Trans. Graph.*, vol. 35, no. 6, p. 224, 2016.
- [17] C. Dai, C. C. L. Wang, C. Wu, S. Lefebvre, G. Fang, and Y.-J. Liu, "Support-free volume printing by multi-axis motion," *ACM Trans. Graph.*, vol. 37, no. 4, pp. 134:1–134:14, July 2018.
- [18] A. V. Shembekar, Y. J. Yoon, A. Kanyuck, and S. K. Gupta, "Generating robot trajectories for conformal three-dimensional printing using nonplanar layers," *Journal of Computing and Information Science in Engineering*, vol. 19, no. 3, p. 031011, 2019.
- [19] K. Xu, L. Chen, and K. Tang, "Support-free layered process planning toward 3 + 2-axis additive manufacturing," *IEEE Transactions on Automation Science and Engineering*, vol. 16, no. 2, pp. 838–850, April 2019.
- [20] C. Wu, C. Dai, G. Fang, Y. J. Liu, and C. C. L. Wang, "RoboFDM: A robotic system for support-free fabrication using FDM," in *2017 IEEE International Conference on Robotics and Automation (ICRA)*, May 2017, pp. 1175–1180.
- [21] T. Chen, L. Zheng, E. Yan, Z. Jiang, T. Moreau, L. Ceze, C. Guestrin, and A. Krishnamurthy, "Learning to optimize tensor programs," in *Advances in Neural Information Processing Systems*, 2018, pp. 3389–3400.
- [22] A. Adams, K. Ma, L. Anderson, R. Baghdadi, T.-M. Li, M. Gharbi, B. Steiner, S. Johnson, K. Fatahalian, F. Durand, *et al.*, "Learning to optimize halide with tree search and random programs," *ACM Transactions on Graphics (TOG)*, vol. 38, no. 4, pp. 1–12, 2019.
- [23] B. T. Lowerre, "The harpy speech recognition system." Ph.D. dissertation, Carnegie Mellon University, Pittsburgh, PA, USA, 1976, aA17619331.
- [24] L. Luo, I. Baran, S. Rusinkiewicz, and W. Matusik, "Chopper: Partitioning models into 3D-printable parts," *ACM Trans. Graph.*, vol. 31, no. 6, pp. 129:1–129:9, Nov. 2012.
- [25] T. Chen and C. Guestrin, "Xgboost: A scalable tree boosting system," in *Proceedings of the 22nd acm sigkdd international conference on knowledge discovery and data mining*, 2016, pp. 785–794.
- [26] Y. Hu, Q. Zhou, X. Gao, A. Jacobson, D. Zorin, and D. Panozzo, "Tetrahedral meshing in the wild," *ACM Trans. Graph.*, vol. 37, no. 4, pp. 60–1, 2018.
- [27] B. McFee and G. R. Lanckriet, "Metric learning to rank," in *Proceedings of the 27th International Conference on Machine Learning (ICML-10)*, 2010, pp. 775–782.
- [28] R. Baeza-Yates, B. Ribeiro-Neto, *et al.*, *Modern information retrieval*. ACM press New York, 1999, vol. 463.
- [29] C. J. Burges, R. Ragno, and Q. V. Le, "Learning to rank with nonsmooth cost functions," in *Advances in neural information processing systems*, 2007, pp. 193–200.
- [30] C. Burges, T. Shaked, E. Renshaw, A. Lazier, M. Deeds, N. Hamilton, and G. Hullender, "Learning to rank using gradient descent," in *Proceedings of the 22nd international conference on Machine learning*, 2005, pp. 89–96.